Norihiro Munetomo for their assistance.

Nomenclature

C_w	= coal concentration	[wt%]
D_p	= particle diameter	[μm]
k	= break down parameter of yield stress defined by Eq. (2)	[Pa^{-1}]
K	= break down parameter of yield stress defined by Eq. (5)	[—]
T	= shear free time interval	[s]
t	= time	[s]
t_h	= half-time of unsteady shear history defined in Fig. 2	[s]
$\dot{\gamma}$	= shear rate	[s^{-1}]
$\dot{\gamma}_{max}$	= maximum shear rate defined in Fig. 2	[s^{-1}]
η	= Bingham plastic viscosity	[Pa·s]
λ_y	= time constant for buildup of yield stress	[s]
τ	= shear stress	[Pa]
τ_y	= Bingham yield stress	[Pa]
τ_{y0}	= yield stress under steady shear flow	[Pa]
$\tau_{y,init.}$	= yield stress at onset of unsteady shear	[Pa]
$\tau_{y\infty}$	= yield stress at the final stage of structure buildup	[Pa]

Literature Cited

1) Alves, G. G., D. F. Boucher and R. L. Pigford: *Chem. Eng. Progr.*, **48**, 385 (1952).
2) Brown, J. P. and K. K. Pinder: *Canad. J. Chem. Eng.*, **49**, 38 (1971).
3) Gillespie, T.: *J. Colloid Sci.*, **15**, 219 (1960).
4) Dinger, B. R., D. F. Funk and J. E. Funk, Sr.: Proc. 4th Int. Symp. Coal Slurry Combustion, Orland (1982).
5) Fredrickson, A. G.: *AIChE J.*, **16**, 436 (1970).
6) Hahn, S. J., T. Lee and H. Eyring: *Ind. Eng. Chem.*, **51**, 856 (1959).
7) Mikami, Y.: *J. Soc. Rheology, Japan*, **8**, 137 (1980).
8) Morgan, R. J.: *Trans. Soc. Rheology*, **12**, 511 (1968).
9) Nagase, Y. and K. Okada: *Funtai Kogakkaishi*, **17**, 392 (1980).
10) Ritter, R. A. and G. W. Govier: *Can. J. Chem. Eng.*, **48**, 505 (1970).

ADSORPTION ISOTHERMS OF HYDROCARBONS AND CARBON DIOXIDE ON ACTIVATED FIBER CARBON

MASAYUKI KURO-OKA, TOSHIYUKI SUZUKI, TOMOSHIGE NITTA AND TAKASHI KATAYAMA

Department of Chemical Engineering, Faculty of Engineering Science, Osaka University, Toyonaka 560

Key Words: Adsorption, Equilibrium, Adsorption Isotherm, Fiber Activated Carbon, Hydrocarbon Gas, Carbon Dioxide

Equilibrium data for single-component adsorption on activated fiber carbon, KF-1500 are presented for the five gases methane, ethane, propylene, 1-pentane and carbon dioxide at 0, 25 and 50°C. An adsorption equation by a multi-site occupancy model for homogeneous surface represents the isotherms fairly well, but the calculated amounts of adsorption are usually less than those observed at low surface coverage. The deviation may be attributed to the surface heterogeneity, which is neglected in the equation. From a comparison of isotherms on glanular and fiber activated carbons, it is suggested that the difference is only in the specific surface area, and that the other two parameters, the number of sites occupied by a molecule and the adsorption equilibrium constant, are almost the same for the two activated carbons.

Introduction

The adsorption equilibrium is one of the fundamental properties for rational design of adsorption equipment such as high-purification columns and solvent recovery systems. Practically useful equations for adsorption isotherms should have the advantage of predicting multi-component adsorptions as well as representing single-component equilibrium data. An adsorption isotherm equation derived from a multi-site occupancy model[1] is considered as one of these equations.

In the present work adsorption equilibrium data of the five gases methane, ethane, propylene, 1-pentane and carbon dioxide on commercial activated fiber carbon, KF-1500, obtained by a gravimetric method

Received February 27, 1984. Correspondence concerning this article should be addressed to T. Katayama. M. Kuro-oka is now with Sanyo Electric Co., Ltd., Osaka 573.

are correlated by means of the multi-site occupancy model. The results are compared with those for granular activated carbon, Nuxit-AL, measured by Szepesy and Illés.[2]

1. Experimental

1.1 Apparatus

A schematic diagram of the adsorption apparatus is shown in **Fig. 1**. Two major parts are an electrobalance A (Cahn, model 1000) and a quartz Bourdon pressure gage D (Texas Instruments, model 145, 1000 mmHg full scale). The precision of weight was 20 μg and the sensitivity of pressure was 0.4 Pa. The Bourdon gage was calibrated with a Ruska air-piston gage. About 0.1 g of adsorbent KF-1500 was activated by heating to 250°C under vacuum over 24 h. Adsorption isotherms at 0, 25 and 50°C were obtained; the temperatures were regulated within $\pm 1/100$°C. The pressure at full evacuation was less than 1 mPa.

Equilibration of adsorption was reached when readings of pressure and weight became constant; this usually took thirty minutes. No hysteresis was observed in several sequences of adsorption and desorption experiments. A buoyancy correction was made for weight measurements. Accuracy of adsorbed mass was 0.2 mg-adsorbate/g-adsorbent.

1.2 Materials

Sample gases except 1-pentane were supplied in commercial cylinders and were used without further purification. Methane (99.97%) and carbon dioxide (99.99%) were from Seitetsu Kagaku Co., Ltd. Ethane (99.7%) was from Takachiho Kagaku Co. and propylene (99.95%) from Sumitomo Chemical Co., Ltd. Pentane, reagent-grade from Nakarai Chemicals Co., Ltd., was degassed and dried with Molecular Sieve 3A. Activated fiber carbon, KF-1500, was given by Toyobo Co., Ltd.

2. Results and Discussion

2.1 Experimental results

Amounts adsorbed (W) on KF-1500 at 0, 25 and 50°C are summarized in **Table 1**, where only sufficient data points for representing each isotherm are shown because of the great number of raw data. Precision of the data is $0.2/M$, where M is the molar mass of adsorbed gas in g·mol^{-1}

Figure 2 shows plots of W against the logarithm of pressure P for three hydrocarbons and carbon dioxide. All the data points for each adsorbate are represented by one curve if appropriate constants are chosen at each temperature to move the abscissa.

Figure 3 shows the log-log plots of W and P for methane, which shows that Henry's law does not hold in the experimental region since the slopes of each isotherm do not approach unity. This may be attributed to the so-called surface heterogeneity with respect to interaction energies. In **Fig. 4** are shown the isosteric heat of adsorption Q_{st} for three adsorbates calculated from the experimental adsorption isotherms. Accuracy of Q_{st} is estimated to be within ± 2 kJ·mol^{-1}. Increases of Q_{st} with decreasing amount of adsorption are observed, indicating that adsorbed molecules at low surface coverage are energetically more stable. The same results are observed for the other two adsorbates. The isosteric heats give direct information for surface heterogeneity.

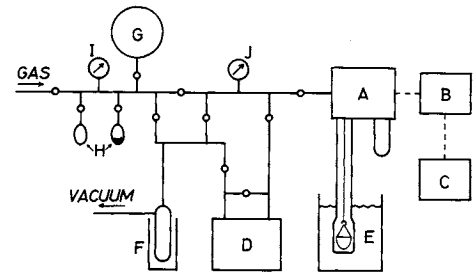

Fig. 1. Schematic diagram of apparatus: A, electrobalance; B, control unit; C, recorder; D, quartz Bourdon gage; E, water bath; F, cold trap; G, gas reservoir; H, liquid source; I, Bourdon gage; J, Pirani gage.

2.2 Simple expression by multi-site occupancy model

An adsorption isotherm for homogeneous surface by the multi-site occupancy model is given as[1]

$$\ln(nKP) = \ln\theta - n\ln(1-\theta) \qquad (1)$$

where θ is the surface coverage; n is the number of active sites occupied by a molecule; K is the adsorption equilibrium constant which represents the interaction between the surface and an adsorbed molecule. Since Eq. (1) assumes no surface heterogeneity, the isosteric heats, Q_{st}, calculated from the model equation are constant against surface coverage for each adsorbent. Therefore, it cannot represent all the experimental results presented in the previous section.

The advantage of Eq. (1) is its simplicity in use. Its applicability to adsorption isotherms on Nuxit-AL, active granule carbon, was discussed in a previous paper.[1] The same method of data reduction is used in the present work.

The surface coverage is calculated as

$$\theta = W/(W^{\bullet}/n) \qquad (2)$$

where $W^{\bullet}$ is the total amount of active sites per gram of adsorbent. **Table 2** summarizes the parameters of n's for each adsorbate and K's for each temperature determined from fits to the experimental values W by means of a non-linear least square method. The solid lines in Figs. 2 and 3 show the isotherms calculated from Eq. (1) with the parameters listed in Table 2. It is noted that the experimental values for W at low surface coverage are greater than the calculated ones,

Table 1. Experimental amounts adsorbed on KF-1500

0°C		25°C		50°C	
P [kPa]	W [mmol/g]	P [kPa]	W [mmol/g]	P [kPa]	W [mmol/g]
		Methane			
0.401	0.039	0.950	0.043	1.511	0.034
0.456	0.045	2.139	0.067	2.181	0.048
1.321	0.085	2.667	0.077	4.447	0.074
2.017	0.133	4.496	0.106	6.573	0.094
3.016	0.142	6.664	0.148	10.05	0.122
5.157	0.225	9.413	0.182	11.71	0.138
6.653	0.257	13.38	0.237	13.40	0.144
9.888	0.355	15.88	0.276	18.26	0.190
13.72	0.439	20.08	0.328	20.03	0.203
17.26	0.519	26.52	0.404	25.18	0.234
21.14	0.578	31.64	0.470	29.55	0.277
26.52	0.701	37.33	0.529	33.63	0.309
31.82	0.782	42.98	0.597	37.02	0.337
35.56	0.862	49.26	0.656	40.30	0.359
40.38	0.930	56.18	0.717	45.13	0.387
53.06	1.125	63.45	0.803	53.65	0.446
63.50	1.274	68.25	0.847	65.07	0.517
72.67	1.398	80.07	0.952	77.88	0.597
86.24	1.564	91.36	1.046	90.46	0.667
99.34	1.709	98.92	1.105	99.07	0.711
		Ethane			
0.0213	0.060	0.0316	0.030	0.0007	0.003
0.0381	0.091	0.115	0.083	0.102	0.032
0.0632	0.136	0.249	0.143	0.181	0.040
0.0840	0.164	0.372	0.196	0.268	0.068
0.145	0.238	0.528	0.246	0.570	0.115
0.244	0.338	0.862	0.337	0.740	0.150
0.410	0.472	1.364	0.476	1.028	0.195
0.596	0.589	1.835	0.574	1.280	0.227
1.028	0.816	2.281	0.655	1.821	0.291
1.881	1.138	2.701	0.743	2.802	0.400
2.631	1.358	3.900	0.918	3.441	0.461
4.206	1.724	5.255	1.097	5.339	0.622
7.637	2.30	8.241	1.415	7.956	0.807
11.91	2.82	11.71	1.698	10.61	0.966
16.55	3.22	18.47	2.15	14.50	1.170
22.61	3.64	26.43	2.56	19.85	1.403
30.32	4.08	38.75	3.04	28.57	1.727
39.82	4.47	51.84	3.44	39.65	2.05
66.59	5.22	79.66	4.06	66.11	2.66
99.19	5.79	100.02	4.38	96.76	3.16
		Propylene			
0.0011	0.069	0.0026	0.026	0.0025	0.007
0.0016	0.089	0.0116	0.103	0.0052	0.015
0.0045	0.168	0.0238	0.178	0.0110	0.030
0.0097	0.279	0.0384	0.242	0.0173	0.048
0.0198	0.411	0.0552	0.300	0.0294	0.074
0.0487	0.652	0.101	0.450	0.0456	0.102
0.113	0.966	0.187	0.613	0.0807	0.162
0.199	1.272	0.283	0.767	0.120	0.216
0.445	1.774	0.623	1.136	0.198	0.306
0.842	2.31	1.157	1.525	0.297	0.394
1.862	3.04	2.181	2.02	0.468	0.522
2.986	3.53	3.115	2.32	0.986	0.799
4.086	3.91	5.609	2.91	1.874	1.108
7.445	4.46	8.527	3.36	3.214	1.459
10.28	4.76	13.31	3.89	6.298	1.984
16.01	5.26	23.72	4.50	10.09	2.41
29.61	5.77	35.98	4.93	16.24	2.90
37.83	5.97	51.16	5.29	27.07	3.44
46.80	6.16	51.89	5.32	41.02	3.89
63.49	6.39	67.56	5.56	66.81	4.42
79.65	6.53	94.12	5.86	99.24	4.83
		1-Pentane			
0.0004	1.295	0.0003	0.409	0.0003	0.197
0.0007	1.422	0.0008	0.667	0.0007	0.320
0.0015	1.708	0.0013	0.844	0.0015	0.440
0.0028	1.940	0.0026	1.047	0.0041	0.694
0.0057	2.33	0.0044	1.262	0.0061	0.783
0.0112	2.68	0.0103	1.611	0.0120	0.998
0.0253	3.07	0.0164	1.838	0.0173	1.123
0.0374	3.23	0.0324	2.17	0.0319	1.353
0.0586	3.43	0.0638	2.54	0.0540	1.599
0.0877	3.61	0.102	2.79	0.0806	1.799
0.130	3.76	0.186	3.09	0.164	2.18
0.188	3.89	0.282	3.30	0.320	2.55
0.327	4.10	0.681	3.67	0.589	2.88
0.490	4.22	1.351	3.93	1.223	3.23
0.906	4.38	2.562	4.15	1.883	3.44
1.545	4.49	4.878	4.31	3.689	3.72
4.402	4.67	7.199	4.39	8.112	4.01
7.360	4.75	14.12	4.52	13.91	4.17
11.82	4.82	19.08	4.57	27.94	4.32
19.03	4.88	30.65	4.64	44.10	4.39
		Carbon dioxide			
0.0906	0.026	0.204	0.025	0.706	0.026
0.148	0.041	0.837	0.067	0.897	0.036
0.428	0.089	1.398	0.099	1.983	0.071
0.555	0.114	2.012	0.141	3.290	0.102
0.807	0.161	2.869	0.181	4.264	0.131
1.495	0.238	3.905	0.237	6.695	0.187
2.418	0.348	5.054	0.288	8.736	0.234
3.291	0.446	6.444	0.346	10.80	0.276
4.060	0.509	9.189	0.463	13.93	0.338
6.686	0.732	14.65	0.660	19.89	0.451
10.87	1.028	19.97	0.831	26.40	0.562
16.57	1.377	26.77	1.022	32.59	0.668
22.48	1.672	34.40	1.221	40.05	0.781
28.97	1.959	46.00	1.491	53.53	0.973
39.83	2.39	58.45	1.753	68.54	1.165
54.77	2.91	68.95	1.957	83.19	1.341
73.08	3.46	83.27	2.21	94.26	1.459
88.38	3.87	96.60	2.41		
96.68	4.07				

mainly due to the surface heterogeneity discussed previously.

The value of 41.5 mmol·g^{-1} for $W^{\bullet}$ of KF-1500 is 33% greater than the value of 31.2 mmol·g^{-1} determined previously for Nuxit-AL.[1] The value of 1440 m^2·g^{-1} for the BET surface area of KF-1500 was obtained by the conventional method, and corresponds to 45.7 mmol·g^{-1} for $W^{\bullet}$ when the carbon surface is assumed to be a graphite structure. Though the BET surface area of Nuxit-AL was not reported by Szepesy and Illés,[2] the value estimated from the assumption that $W^{\bullet}$ is proportional to the BET surface is 1100 m^2·g^{-1} for Nuxit-AL, which is

Table 2. Parameters determined from single-component adsorption isotherms on KF-1500

Component	n	K [MPa^{-1}] 0°C	25°C	50°C	Av. dev. [mmol·g^{-1}]	A_p [nm^2]
CH_4	4.23	0.893	0.441	0.246	0.019	0.126
C_2H_6	3.74	18.8	6.73	2.85	0.081	0.187
C_3H_6	4.28	223.	67.1	21.3	0.092	0.243
1-C_5H_{12}	6.55	2.28×10^5	3.11×10^4	6.20×10^3	0.072	0.375
CO_2	3.04	2.78	1.12	0.548	0.044	0.134

$W^\bullet = 41.5$ mmol·g^{-1}.

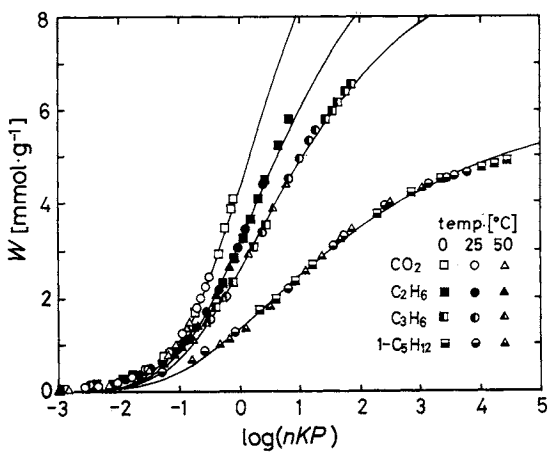

Fig. 2. Adsorption isotherms on KF-1500.

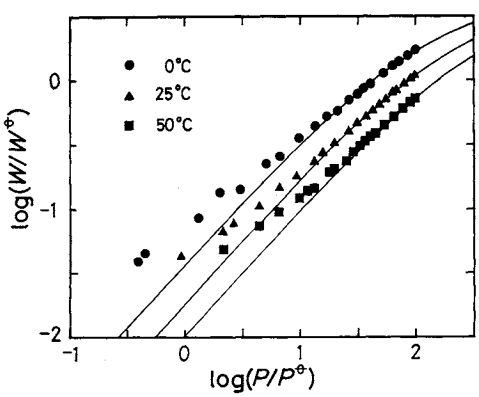

Fig. 3. Adsorption isotherms of methane on KF-1500 ($P^\ominus = 1$ kPa, $W^\ominus = 1$ mmol·g^{-1}).

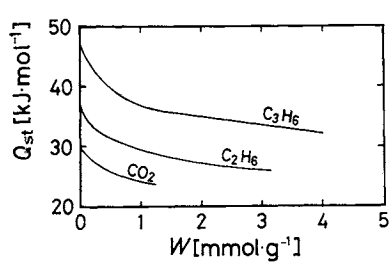

Fig. 4. Isosteric heats of adsorption on KF-1500 at 25°C.

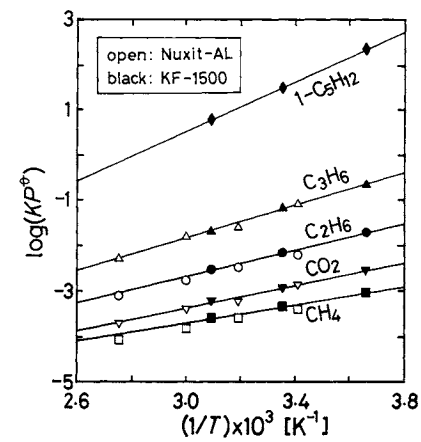

Fig. 5. Adsorption equilibrium constants against reciprocal of T ($P^\ominus = 1$ kPa).

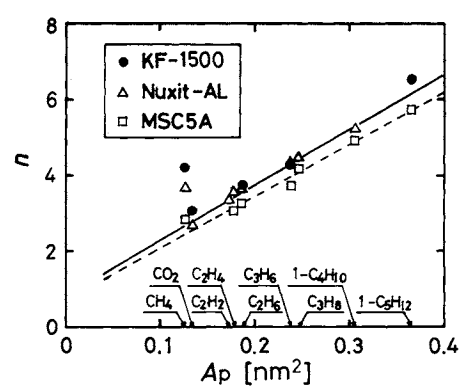

Fig. 6. Relationship between parameter n and molecular area projected on a plane.

reasonable for a granular activated carbon.

Figure 5 shows the temperature dependence of K where the open and the filled keys represent Nuxit-AL and KF-1500, respectively. The parameter n is correlated in **Fig. 6** against the molecular area, A_p, projected on a surface where a molecule lies in its stable position. The solid line in Fig. 6 is expressed as

$$n = 14.44 A_p / A^\ominus + 0.90 \qquad (3)$$

where $A^\ominus = 1$ nm^2.

Since Eq. (1) is a simplified expression for real complex systems, values of the parameters are slightly changeable according to the region of data points available in the least-square determination. It is interesting, however, to see in Figs. 5 and 6 good correlations of the parameters, K and n, obtained for the two active carbons, KF-1500 and Nuxit-AL.

Concluding Remarks

The adsorption equation for homogeneous surface, Eq. (1), can represent single-component isotherms of hydrocarbons and carbon dioxide on activated fiber carbon KF-1500 fairly well, but systematic deviations were observed in regions of low surface coverage. The total amount of active sites $W^{\bullet}$ may be an adsorbent property which is proportional to the specific surface area. The value of $W^{\bullet}$ for KF-1500 is 33% greater than that of Nuxit-AL, an activated granular carbon. The obtained parameters n and K are almost the same for the two activated carbons.

The isosteric heats of adsorption calculated from the experimental isotherms decrease with increasing surface coverage for the five adsorbates on KF-1500. The curves of the isosteric heat indicate that the surface is a little heterogeneous. These observations are compatible with systematic deviations between the calculated and the experimental adsorptions.

Acknowledgment

The authors are grateful to Toyobo Co., Ltd. for providing the activated fiber carbon KF-1500.

Nomenclature

A_p	=	molecular cross-sectional area	[nm^2]
K	=	adsorption equilibrium constant	[Pa^{-1}]
M	=	molar mass	[g·mol^{-1}]
n	=	number of sites occupied by a molecule	[—]
P	=	pressure	[Pa]
Q_{st}	=	isosteric heat of adsorption	[J·mol^{-1}]
T	=	temperature	[K]
W	=	amount adsorbed per gram of adsorbent	[mol·g^{-1}]
$W^{\bullet}$	=	amount of sites per gram of adsorbent	[mol·g^{-1}]
θ	=	surface coverage	[—]

Literature Cited

1) Nitta, T., T. Shigetomi, M. Kuro-oka and T. Katayama: *J. Chem. Eng. Japan*, **17**, 39 (1984).
2) Szepesy, L. and V. Illés: *Acta Chim. Hung.*, **35**, 37 (1963); *Acta Chim. Hung.*, **35**, 53 (1963).

BUBBLE FORMATION PATTERN WITH WEEPING AT A SUBMERGED ORIFICE

TOSHIRO MIYAHARA, MINORU IWATA AND TERUO TAKAHASHI
Department of Industrial Chemistry, Okayama University, Okayama 700

Key Words: Fluid Mechanics, Bubble Formation Regime, Weeping, Single Orifice, Transitional Point

Bubble formation phenomena with weeping at a submerged orifice were investigated experimentally over a range of orifice diameters of 3–13.2 mm. There appeared to be four regimes of interest: single bubbling at small chamber volumes and low gas flow rates, doubling noticed with increasing gas flow rate, jetting at further increase of gas flow rate and pairing at very large chamber volumes under conditions of gas flow rates smaller than those for jetting point. Empirical relationships predicting each transitional point of bubble formation regimes are obtained.

Introduction

Gas-liquid contacting devices such as bubble and plate columns are very widely used for the transfer of matter or heat across an interface in the chemical industry. In such devices perforated plates, which serve for the dispersion of gases, have been widely used because of their simple structure.

As is well-known, weeping through the perforations of perforated plates, usually undesirable, occurs with relatively large hole diameters and low gas flow rates during bubble formation.[2,7] It does not occur on plates with small hole diameters and operation at very large gas flow rates.

To clarify the gas-liquid contacting mechanism, the phenomena of bubble formation from single holes have been extensively studied. Numerous studies have been made of the formation of gas bubbles under conditions where weeping has not occurred.[3,6]

McCann *et al.*[4] have studied bubble volume and weeping rate theoretically, using potential flow analysis. However, in their work, supporting data were presented for the air–water system only in the range of large gas flow rates where the phenomena of pairing or doubling mentioned below might occur. More recently, Akagi *et al.*[1] have examined the

Received March 23, 1984. Correspondence concerning this article should be addressed to T. Miyahara. M. Iwata is now with Kao Corporation, Tokyo 103.